



Conformal coating by liquid route on three-dimensional topology

Nathalie Poirot^{1,a}, Thomas Tillocher², and Pierre-Ivan Raynal³

¹ GREMAN-IUT de Blois, 15 rue de la Chocolaterie, 41000 Blois Cedex, France

² GREMI, CNRS/Université d'Orléans, 14 rue d'Issoudun, 45067 Orléans, France

³ Plateforme IBiSA de Microscopie Electronique, Université de Tours, 10 bd Tonnellé, BP 3223, 37032 Tours Cedex, France

Received 14 January 2022 / Accepted 9 April 2022 / Published online 9 May 2022

© The Author(s), under exclusive licence to EDP Sciences, Springer-Verlag GmbH Germany, part of Springer Nature 2022, corrected publication 2022

Abstract We demonstrated a new approach to the production of three-dimensional-coated patterns using the liquid route. Metallic perovskite oxides were coated onto three-dimensional (3D) micro-structured substrates with different aspect ratios. The method's success relies on the solution viscosity being adjusted by adding viscous liquid. The process of oxide thin films follows three stages: preparing the precursor solution, coating the solution by spin-coating process onto three-dimensional-Si substrates, and post-annealing. Chemical solution 3D-coating is conformal.

1 Introduction

Over the last few years, miniaturized power source development and device diversification increased the need for three-dimensional (3D) integration. As an example, components such as Metal/Insulator/Metal (MIM) and Micro-Electro-Mechanical-Systems have been developed with 3D integration to be embedded into chips. These 3D-developed components have also been widely developed for applications such as Dynamic Random Access Memory [1–3] and optical or Radio-frequency (RF) switches [4–6]. The benefits of 3D architectures are reductions in size and cost, increase in reliability and energy-related performance.

Moreover, 3D structuring improves the physical properties of devices. Therefore, research in this area is extremely active, particularly in the fields of micro-batteries, supercapacitors, fuel cells and solar cells [7–21]. A significant breakthrough was achieved by Golodnitsky [10] in the field of Li-ion microbatteries by reaching a reversible capacity of 3.5 mA·h/cm². This is about 20 to 30 times superior to the two-dimensional (2D) thin films capacity. In the area of RF applications, the integration of functions requires a more complex grouping of active and passive components.

Current deposition techniques for growing thin films on 3D substrates are divided into two categories: physical and chemical. Physical techniques consist of Physical Vapor Deposition (PVD), vacuum evaporation, molecular beam epitaxy and sputtering. These techniques require combining (high voltage, vacuum, etc.)

and low deposition rates (close to 10 nm·min⁻¹). Chemical techniques consist of electro-deposition by electrophoresis, Chemical Vapor Deposition, plasma-activated chemical vapor deposition, Plasma-Enhanced Chemical Vapor Deposition and atomic layer deposition (ALD).

When depositing complex perovskite-type oxide films on high aspect ratio 3D structures, the conventional liquid route becomes inefficient: the capillary process increases proportionally with the aspect ratio, which is defined by the etching depth divided by the trench width. To obtain a good coating on 3D micro-structured substrates with a high aspect ratio, the viscosity control of deposit solution is the critical parameter.

To control the solution viscosity, concentration is the only parameter to be adjusted. Indeed, the capillary process follows Jurin's law (Eq. 1):

$$h = \frac{2\gamma \cos \theta}{r\rho g}, \quad (1)$$

where h is the liquid height, γ is the liquid surface tension, θ is the liquid contact angle on the substrate, ρ is solution density, r is the tube radius and g is gravitational acceleration.

The contact angle must be controlled by the solvent choice and/or by the addition of additives allowing good wettability with silicon (Si) substrates.

In this paper, we demonstrate how controlling the solution viscosity before coating makes 3D conformal liquid coating on Si substrates efficient whatever the aspect ratio values are.

We report the preparation of LaNiO₃ (LNO) films on 3D-Si substrates. The LNO component has been cho-

^a e-mail: nathalie.poirot@univ-tours.fr (corresponding author)

sen because of its good electrical conductivity. It could be used as bottom and top electrodes in MIM, electrodes in ferroelectric devices and in integrated capacitors or buffer layers [22–27]. A chemical solution deposition process has been selected to prepare the LNO thin films. Until now, the deposition of LNO thin films prepared by the chemical solution deposition process onto 3D substrates has rarely been successfully investigated.

The obtained results demonstrate that chemical solution deposition makes possible efficient coating of 3D micro-structured substrates with high aspect ratios.

2 Materials and methods

2.1 Characterization

The solution viscosity was checked using a Brookfield viscometer (LVD-III) with a cone spindle. Thermogravimetric analyses (Perkin Elmer Diamond thermogravimetry (*TG*) and differential thermal analysis (*DTA*) of dried precursors were performed at a ramp rate of $10\text{ }^{\circ}\text{C}\cdot\text{min}^{-1}$ from room temperature to $1000\text{ }^{\circ}\text{C}$, using $\alpha\text{-Al}_2\text{O}_3$ as a reference. Resistivity measurements on films were carried out using the four-probe method.

The morphology of coated films was characterized by scanning electron microscopy (SEM). The SEM micrographs were acquired on a ZEISS ULTRA Plus field emission (FE)-SEM at a low accelerating voltage (2–5 kV) and short working distance (2–3 mm) with the InLens secondary electron detector. Structural analysis was investigated by X-ray diffraction (XRD) (Bruker D8 Advanced model with twin-twin type).

2.2 Methods

The method consists of simply dissolving the metallo-organic compounds in solvents [22, 23]. No hydrolysis of precursors is observed. The species in the solution are a simple mixture of the starting molecules. The four steps below were followed:

1. Precursors are dissolved in a suitable solvent and mixed in stoichiometric proportions.
2. The obtained solution is coated on a substrate by spin-coating.
3. To remove the solvent and produce an inorganic film, thermal processing is applied to the as-deposited film.
4. The samples are annealed up to the oxide crystallization temperature.

Precursors are tetra-hydrated lanthanum nitrate (Sigma Aldrich, $\text{La}(\text{NO}_3)_3 \cdot 6\text{H}_2\text{O}$, 99.9%) and nickel acetate (Sigma Aldrich, $\text{Ni}(\text{OOCCH}_3)_2 \cdot 4\text{H}_2\text{O}$, 99.9%), the solvent is 2-methoxyethanol (Sigma Aldrich, $\text{C}_3\text{H}_8\text{O}_2$, 99.9%). Glycerol (Sigma Aldrich, 99–101% purity) and poly(ethylene glycol) (PEG) – 10,000 (Sigma Aldrich) are added to the LNO solution to adjust the viscosity.

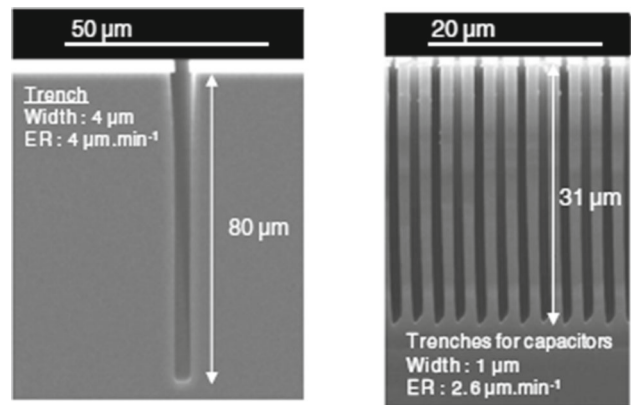


Fig. 1 Cross-sectional SEM micrograph of typical trench profiles obtained in silicon cryoetching (cf. Dussart 2014)

The prepared concentrations without PEG and glycerol are 0.15 M, 0.3 M and 0.5 M. The solvent choice is essential to obtain a dense thin film. The 2-methoxyethanol solvent has been selected for two reasons. The first is the presence of glycol groups that allow a strong affinity with metal atoms of tetra-hydrated lanthanum nitrate and nickel acetate, so that a good combination with La^{3+} and Ni^{2+} atoms is obtained. As a result, no precipitation is observed during solvent evaporation. The second reason is the high wettability of 2-methoxyethanol on (Si) substrates.

To synthesize the precursor solution, the lanthanum nitrate is dissolved in the solvent, preheated at $100\text{ }^{\circ}\text{C}$ to evaporate residual water, under constant stirring. When maintaining heating at $80\text{--}90\text{ }^{\circ}\text{C}$, the solution becomes clear. An equimolar amount of nickel acetate is then added. After 30 min of stirring, the solution becomes homogeneous. The viscosity values increase with concentration. These are 2.8 mPa.s, 4.41 mPa.s and 9.8 mPa.s, respectively.

The solutions with added PEG or glycerol have a mass ratio ($m_{\text{LNOsolution}}/m_{\text{adjuvant}}$) that varies from 1 to 4. The respective viscosity values are then close to $40\text{ mPa}\cdot\text{s} \sim 85\text{ mPa}\cdot\text{s}$.

The same procedure has been used by Vincent et al. for precursor solution preparation with polyester addition without PEG or glycerol [28]. For adjusting the viscosity, Gabard et al. have added Si nanoparticles the same polymer [29].

2.3 Substrate preparation

To achieve high aspect ratio structures on Si (110) substrates, standard cryogenic etching [30] or STiGer [31] are used. The latter is a time-multiplexed cryogenic etching method using SF_6 or SF_6/O_2 plasmas. This technique combines advantages of both the Bosch and standard cryogenic processes. Trenches and vias with different aspect ratios are thus obtained. SEM pictures of typical high-aspect-ratio trenches produced through the standard cryogenic etching are shown in Fig. 1.

Cleaning the Si substrate before a coating is performed in two steps:

1. removal of chemical residues through immersion in 40% wt. HF solution
2. Radio Corporation of America (RCA) method [33]; The Si substrates are immersed for 10 min in a mixture in a mixture of H₂O, H₂O₂ and NH₄OH with a volumetric ratio of 5:1:1 and heated at about 75–80 °C.

2.4 Coating process

The coatings on clean Si substrates are performed using spin-coating with a ramp rate of 2000 rpm/s and a spin speed of 3000 rpm for 30 s at ambient temperature in air. 150 µL of solution are deposited on etched Si substrates.

After the coating, all samples obtained are heated in air at precisely defined temperatures following three steps:

1. Drying at 175 °C on a hot plate for 2 min to allow solvent evaporation.
2. Pyrolyzing at 375 °C on a hot plate for 3 min to remove the metal-organic matrix.
3. Calcination of films inserted directly into a furnace preheated at 700 °C with a dwell time of 20 min to crystallize and densify the films, i.e. rapid thermal annealing (RTA) process.

For determining the required temperature values, the thermal behaviors of solutions have been studied. In Fig. 2, the evolution of percentage weight loss with temperature is shown for glycerol, PEG and LaNiO₃ solutions. The data indicate that the glycerol and PEG have decomposition temperatures close to 180 °C and 250 °C, respectively, while the 2-methoxyethanol is decomposed above 200 °C. LNO crystallization temperature is about 650 °C. In the third heating step, thermal process is called RTA although it is not a “true” RTA where the ramp temperature can be close to 100 °C/s.

Two major benefits of the RTA operation are:

1. limitation of the diffusion phenomena to the interface
2. film densification without cracks.

The complete process must be repeated as many times as the desired number of layers.

3 Results and discussion

Three methods have been used to coat a 3D-substrate with a LaNiO₃ thin film. We report here the results for each of them.

3.1 Coating with non-modified LaNiO₃ chemical solution

A stable precursor chemical solution of LaNiO₃ was first prepared and used for coating according to previously reported chemical solution deposition processes. A single coated layer was deposited, the solution viscosity being about 9.8 mPa.s and with a 0.5 M LNO concentration. The cross-sectional SEM micrograph of LNO film on Si substrate is shown in Fig. 3. The LNO layer is dense, but many cracks are observed. Film thickness varies from the bottom to the top of the trench. Non-covered parts, accumulations of products and filament formation in the trenches are observed. These defects were systematically observed for a coated-solution viscosity value below 10 mPa.s., no matter what the precursor concentrations were.

As described by Seemann et al. the wetting of microstructured surfaces depends on many factors [33]. From this work, a global morphology diagram is derived (see Fig. 4). For high aspect ratios, as in our case, the system corresponds to the filament regime (F⁻) with a negative Laplace pressure. The cross-sectional SEM micrograph for a coating with a 0.15 M LNO solution with high aspect ratios (8) is shown in Fig. 4c. The filaments are well visible. The higher the aspect ratios are, the more complex uniform trench coating becomes. As stated by [31], a homogeneous coating is impossible on geometries showing breaks of angles. As indicated before, the capillary force follows Jurin’s law. The solution viscosity is one of the parameters that can be modified to reduce the capillary force and therefore obtain uniform coating in trenches. Consequently, the solution viscosity must be increased. As a consequence, PEG and glycerol have been added to the LNO solution, with good wettability of the chemical solution on the Si substrate for LNO film coating.

3.2 Coating modified LaNiO₃ chemical solution

Consequently, new stable precursor chemical solutions of LaNiO₃ have been prepared as previously described with the addition of glycerol or PEG to obtain viscosity values between 40 and 70 mPa.s. Figure 5 shows the cross-sectional SEM micrograph for one deposited layer with a 0.3 M (LNO+ PEG) solution concentration. The aspect ratio is 8 and the viscosity value 40 mPa.s.

Cracks are observed in the trench bottom and the trench walls are non-uniformly covered with the formation of filaments. The middle trench walls are generally not covered by oxide material. Whatever the concentration value and the mass ratio ($m_{\text{LNOsolution}}/m_{\text{adjuvant}}$) are, the same results are observed when the viscosity value is down to 70 mPa.s. Our results confirm the morphology diagram published by Seemann et al. [33] and reported in Fig. 4.

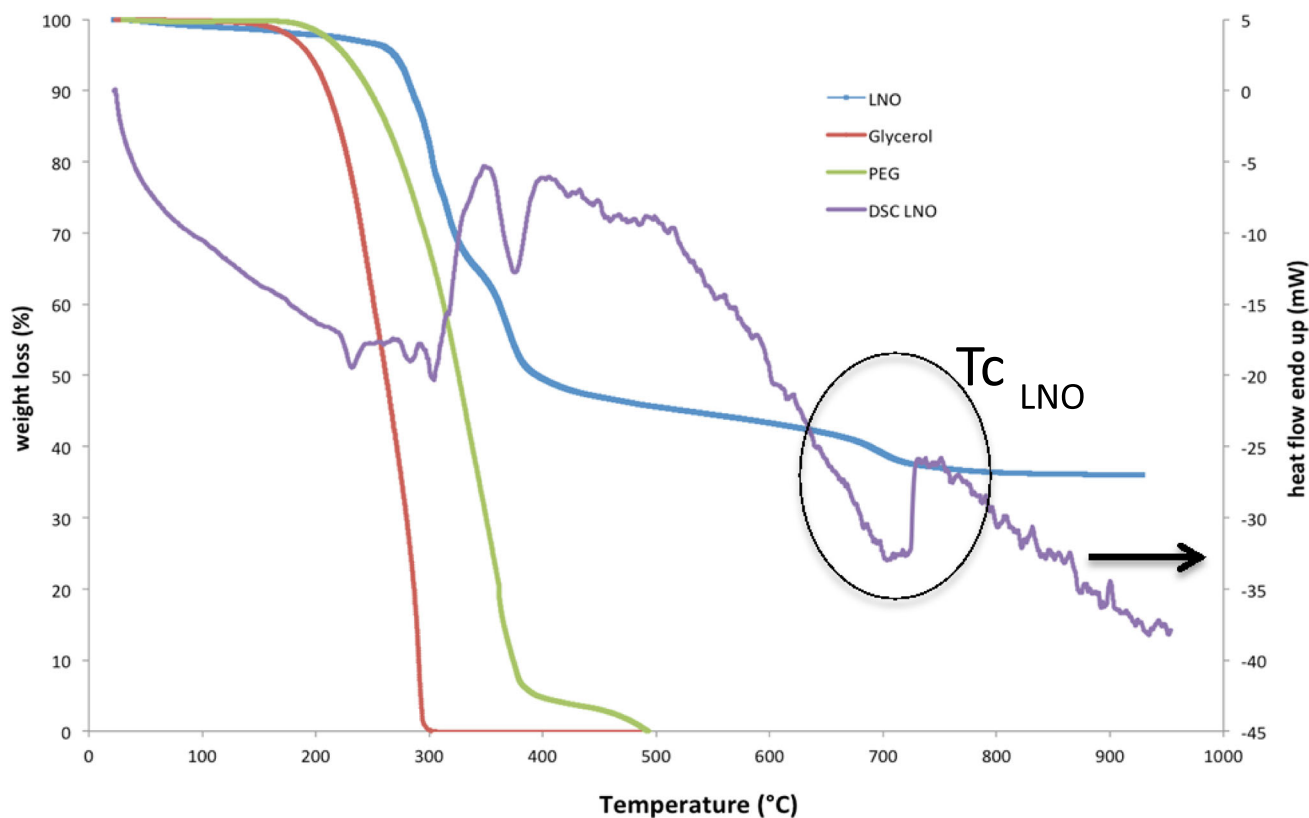
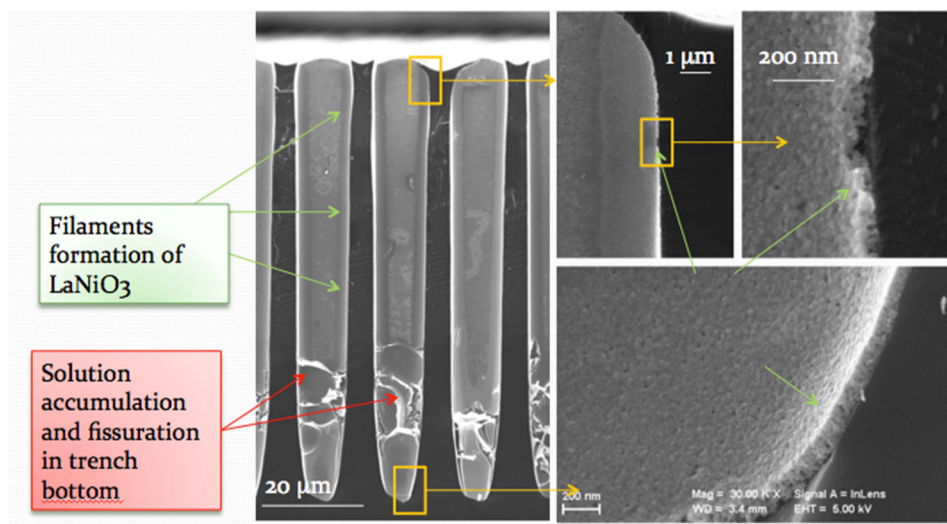


Fig. 2 Thermal analysis of LaNiO_3 solution, glycerol and PEG. T_{cLNO} : crystallization temperature of LNO

Fig. 3 Cross-sectional SEM micrograph of a LaNiO_3 coating in trench with a 0.5 M



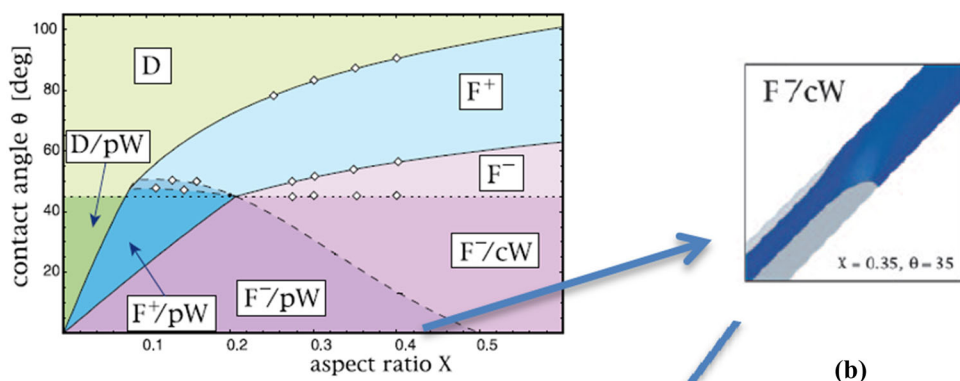
3.3 Coating modified LaNiO_3 chemical solution with viscosity values above $70 \text{ mPa} \cdot \text{s}$

The solution viscosity can be increased by modifying the mass ratio between LNO solution and adjuvant. A new stable and homogeneous mixture with 1 mL of 0.6 M LNO and 1 mL of PEG has been prepared. Viscosity value is close to $85 \text{ mPa} \cdot \text{s}$. A single layer has been coated on trenched Si substrate with an aspect ratio close to 3. The cross-sectional SEM micrographs

are displayed in Fig. 6. No cracks or filaments, as predicted by Wi et al. [23], were observed and the LNO material was dense. The bottom trench was well covered, with a LNO thickness close to 45 nm. The coating is homogeneous with precipitation in the trenches. By comparison, the LNO thickness on a 2D surface is close to 31 nm with the same LNO solution concentration as used for 3D substrates.

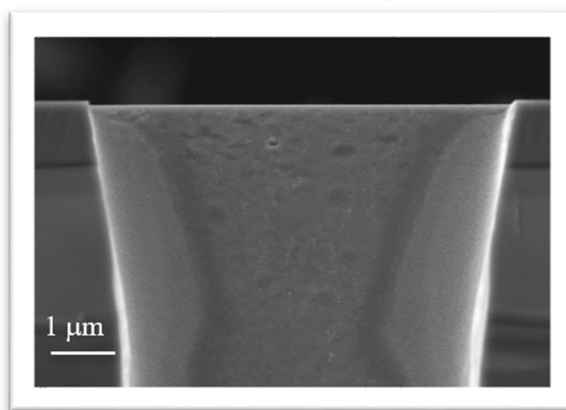
The layer thickness is controlled by the LNO solution concentration, independently of glycerol or PEG

Fig. 4 Morphology diagram as a function of groove aspect ratio X (a) and material contact angle θ (b), reproduced with permission from Seemann [33]. Key: \pm = Laplace pressure, F=Filament, cw=corner wedges, D = droplet, pw=pinned wedges. Cross-sectional SEM micrograph for a coating with a 0.15 M LNO solution with high aspect ratio of 8



(a)

(b)



(c)

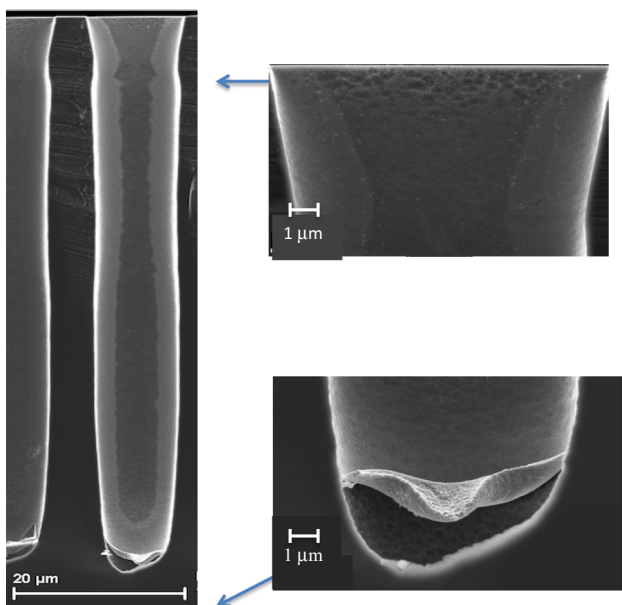


Fig. 5 Cross-sectional SEM micrograph of (0.3 M LNO solution + PEG) coating with a viscosity value of 40 mPa.s

addition. Electrical resistivity of 3D LNO film is about $2.4 \text{ m}\Omega\cdot\text{cm}^2$, a value close to those measured for the 2D LNO thin films. XRD pattern (see Fig. 7) shows that LNO thin films exhibited a single perovskite cubic phase with preferred-(1 1 0) orientation. This orientation was kept layer by layer if each deposited layer remained thicker than 100 nm [34]. The addition of PEG did not affect the oriented LNO growth.

To validate this process, multi-layers coating has been experimented. A mixture was prepared with a 0.3 M LNO solution and PEG with a mass ratio close to 1. The solution viscosity was about 80–85 mPa.s. The SEM results of three layers coated on a Si substrate with an aspect ratio about 10 are shown in Fig. 8.

The coating is uniform, and no cracks are observed. However, many defects can be noted: they do not relate to the coating process. As it happens, when cutting Si substrate, some ceramic piece residues have fallen into the trenches. Figure 8 shows that successive LNO layers with no defects can be obtained when the viscosity value is about 80–85 mPa.s.

Another solution mix was studied: 1 mL of 0.6 M LNO solution mixed with 1 mL of glycerol. The viscosity was close to 80 mPa.s. After homogenization of the mixture, the system was deposited as a single layer on substrates with an aspect ratio of about 3. Figure 9 shows the cross-sectional SEM micrographs. The thin films are porous due to the decomposition of glycerol.

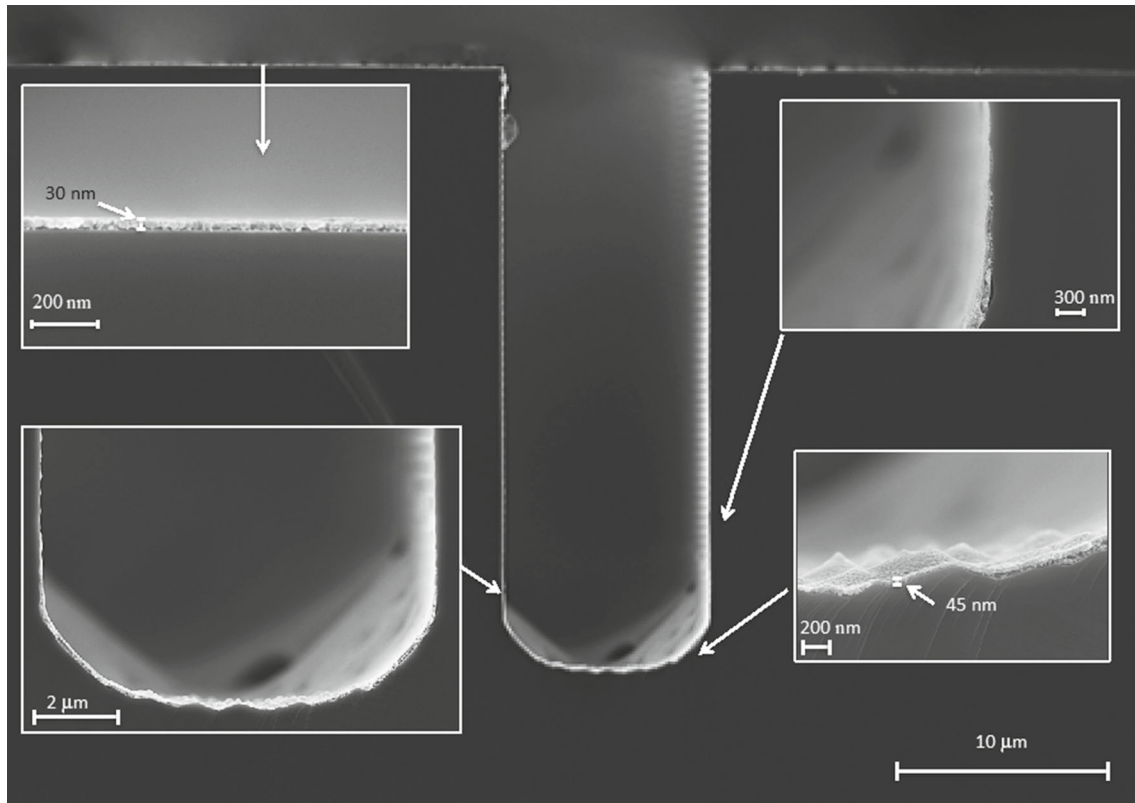
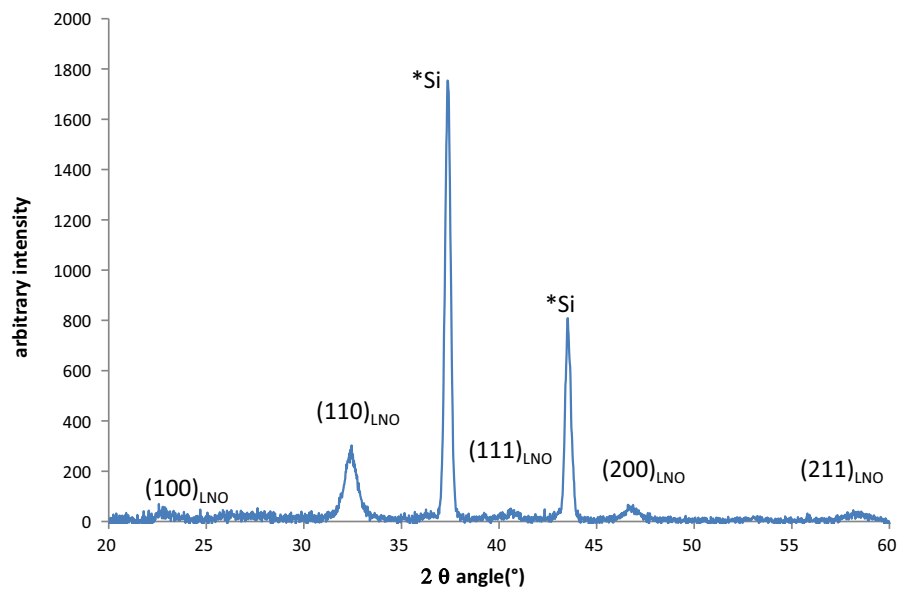


Fig. 6 Cross-sectional SEM micrograph obtained from a layer of a (1 mL PEG + 1 mL 0.6 M LNO) solution. The aspect ratio is 3

Fig. 7 DRX on LNO films grown following a preferred orientation along (110)



Consequently, the electrical conductivity could not be measured. The 3D-substrate is covered with the LNO ceramic with a thickness close to 200 nm. Edges are well covered too, with regular thickness. The bottom trenches exhibit an irregular surface but are also well covered. In conclusion, the covering is uniform.

Table 1 synthesizes the results obtained when changing the various parameters: adjuvant used, viscosity level, aspect ratio, number of coated layers.

Fig. 8 Cross-sectional SEM micrograph obtained from 3 layers of a 0.3M (PEG + LNO) solution heating at 700 °C. The Si aspect ratio is 10

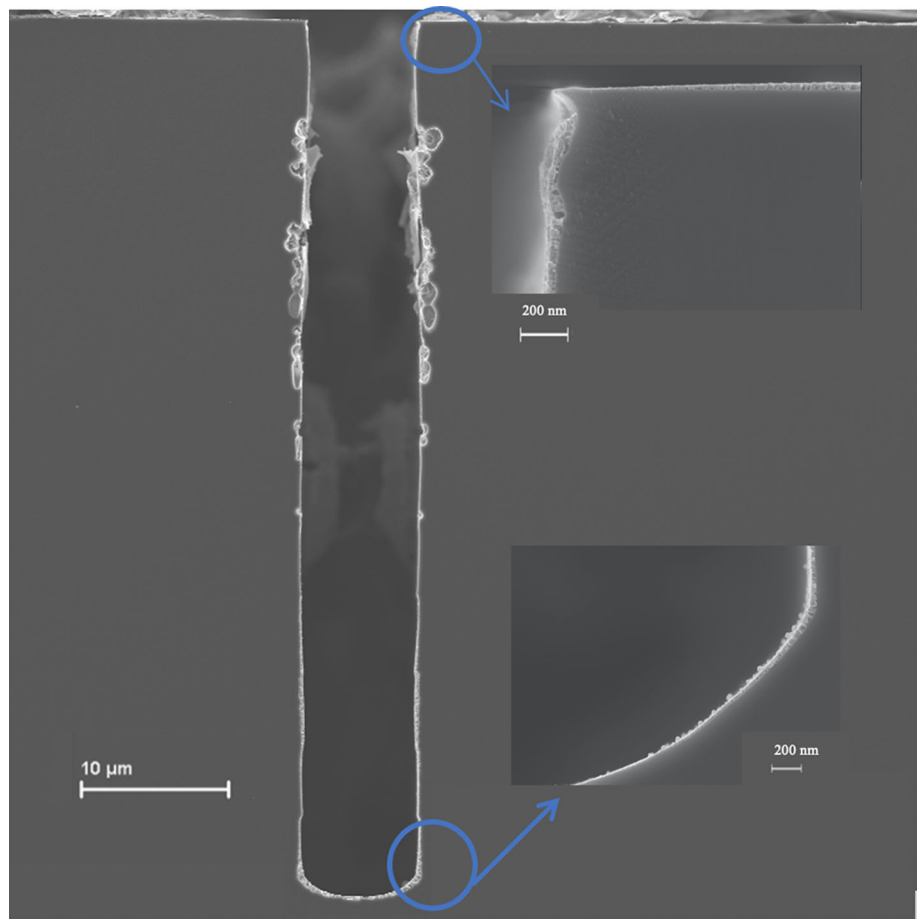


Fig. 9 Cross-sectional SEM micrographs obtained with a (Glycerol+LNO) mixture for a single deposited layer. **a** Image on the edge of the trench, **b** image of the layer on the surface, **c** image in the trench bottom

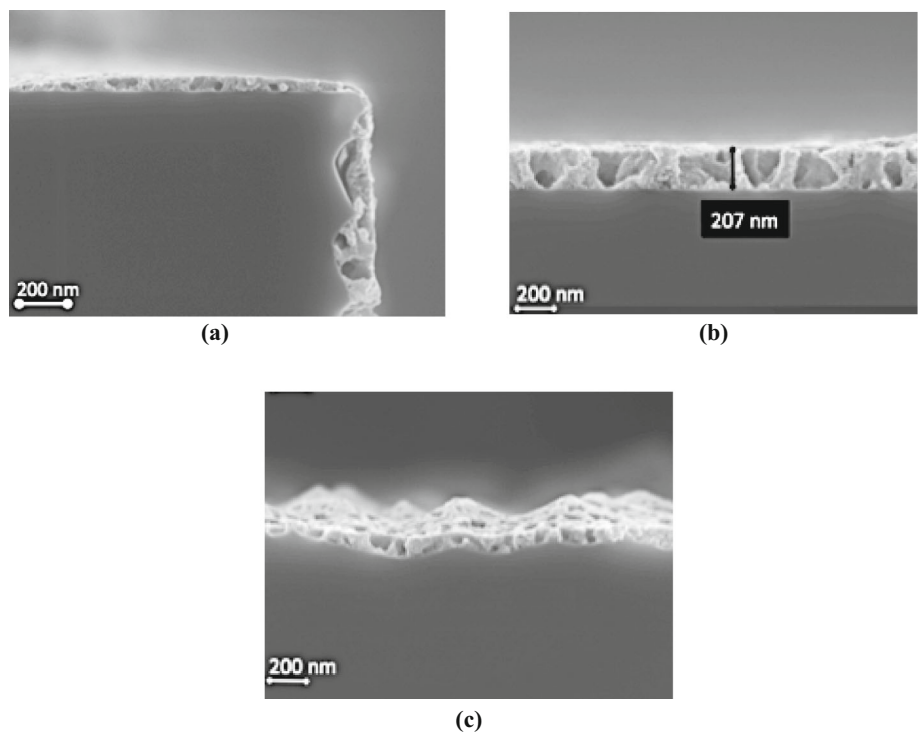


Table 1 Coating quality as a function of different parameters

| Solution concentration | Adjuvant used | Viscosity | Aspect ratio | Layers number | Coating quality | Figure number |
|------------------------|---------------|-----------|--------------|---------------|-----------------|---------------|
| 0,5 | None | 9,8 | 9 | 1 | None | 3 |
| 0,15 | None | 2,8 | 8 | 1 | None | 4 |
| 0,3 | PEG | 39 | 8 | 1 | None | 5 |
| 0,6 | PEG | 85 | 3 | 1 | Good | 6 |
| 0,3 | PEG | 85 | 10 | 3 | Good | 8 |
| 0,6 | Glycerol | 80 | 3 | 1 | Good | 9 |

4 Conclusions

In this work, we demonstrate that coating 3D micro-structured substrates with chemical solutions is possible without going through expensive techniques such as PVD or CVD for example. A control of the solution viscosity is necessary for obtaining a homogeneous solution and a good wettability of the solution on a Si substrate. Table 1 synthesizes the results obtained when tweaking the various parameters: adjuvant used, viscosity level, aspect ratio, number of layers.

Our experimental results demonstrate that solution viscosity control is the essential parameter to obtain uniform coating on 3D micro-structured substrates with various aspect ratios.

Moreover, our experiments highlight a new coating method for complex oxides deposited on 3D-structured substrates. Our process is less complex and less expensive than the physical (PVD) and chemical (ALD) ones. Indeed, it combines chemical solution synthesis with spin-coating deposition. It exhibits the following advantages: high solution stability, good wettability on Si substrates, simplicity, speed and low cost. This process also does not require high vacuum or high-temperature levels.

The key success factors of this process are:

1. a solution viscosity value equal to or greater than 80 mPa.s
2. heating of the substrates up to 350 °C without degradation
3. a large choice of materials:
 - for 3D structured substrates: Ceramics (Al_2O_3 , *Yttria-stabilized zirconia*, etc.), metals (Ni, Fe, etc.), semiconductors (Si, etc.), glass (silica), or mixtures (ceramics, composites, etc.), solar cells.
 - for deposited oxides: TiO_2 , V_2O_5 , RuO_2 , CoO_2 , NiO, ZnO, CeO_2 , ABO_3 perovskite, A_2BO_4 double-perovskite, etc.

This new coating method opens a new perspective in 3D integrated devices as biomedical implants, sensors or integrated circuits and small size integrated batteries. By enlarging the specific surface, 3D-integrated devices offer high-level physical properties compared to 2D-integrated devices. The advantages of the developed process are simplicity, speed, low cost, air pressure. High pressure and temperature levels are not

required in comparison with the classical coating thin films methods.

Acknowledgements This research project was supported through funding from the ANR (French National Research Agency).

Declarations

Conflict of interest The authors declare that they have no conflict of interest.

References

1. J.H. Klootwijk, K.B. Jinesh, W. Dekkers, J.F. Verhoeven, F.C. Van den Heuvel, H.D. Kim, D. Blin, M.A. Verheijen, R.G.R. Weemaes, M. Kaiser, J. Ruigrok, F. Roozeboom, Ultrahigh capacitance density for multiple ALD-grown MIM capacitor stacks in 3-D silicon. *IEEE Electron Device Lett.* **29**, 740–742 (2008)
2. B.L. Ellis, P. Knauth, T. Djenizian, Three-Dimensional self-supported metal oxides for advanced energy storage. *Adv. Mater.* **26**, 3368–3397 (2014)
3. J.H. Klootwijk, K.B. Jinesh, F. Roozeboom, MIM in 3D: Dream or reality? *Engineering* **8**, 1507–1513 (2011)
4. J.B. Bates, N.J. Dudney, D.C. Lubben, G.R. Gruzalski, B.S. Kwak, X. Yu, R.A. Zuhr, Thin-film rechargeable lithium batteries. *J. Power Sources* **54**, 58–62 (1995)
5. J.F.M. Oudenhoven, L. Bagetto, P.H.L. Notten, All-solid-state lithium-ion microbatteries: a review of various three-dimensional concepts. *Adv. Energy Mat.* **1**, 10–33 (2011)
6. J.F.M. Oudenhoven, T. van Dongen, R.A.H. Niessen, M.H.J.M. de Croon, P.H.L. Notten, Low-pressure chemical vapor deposition of LiCoO_2 thin films: a systematic investigation of the deposition parameters. *J. Electrochem. Soc.* **156**, 69–174 (2009)
7. L. Bagetto, R.A.H. Niessen, F. Roozeboom, P.H.L. Notten, High energy density all-solid-state batteries: a challenging concept towards 3D integration. *Adv. Funct. Mater.* **18**, 1057–1066 (2008)
8. B. Asbani, G. Buvat, J. Freixas, M. Huvé, D. Troadec, P. Roussel, T. Brousse, C. Lethien, Ultra-high areal capacitance and high rate capability RuO_2 thin film electrodes for 3D micro-supercapacitors. *Energy Storage Mater.* **42**, 259–267 (2021)
9. N. A. Kyeremateng, T. Brousse, D. Pech, Microsupercapacitors as miniaturized energy-storage components for on-chip electronics. *Nat. Technol.* **12**, 7–15 (2017)

10. E. Eustache, C. Douard, A. Demortière, V. De Andrade, M. Brachet, J. Le Bideau, T. Brousse, C. Lethien, High areal energy 3D-interdigitated micro-supercapacitors in aqueous and ionic liquid electrolytes. *Adv. Mater. Technol.* **2**, 1700126 (2017)
11. E. Eustache, P. Tilmant, L. Morgenroth, P. Roussel, G. Patriarche, D. Troadec, N. Rolland, T. Brousse, C. Lethien, Silicon-Microtube Scaffold Decorated with Anatase TiO₂ as a Negative Electrode for a 3D Lithium-Ion Microbattery. *Adv. Energy Mater.* **11**, 1301612 (2014)
12. H. Mazor, D. Golodnitsky, L. Burstein, A. Gladkich, E. Peled, Electrophoretic deposition of lithium iron phosphate cathode for thin-film 3D-microbatteries. *J. Power Sources* **198**, 264–272 (2012)
13. D. Golodnitsky, M. Nathan, V. Yufit, E. Strauss, K. Freedman, L. Burstein, A. Gladkich, E. Peled, Progress in three-dimensional (3D) Li-ion microbatteries. *Solid Ionics State* **177**, 2811–2819 (2006)
14. T. Liu, H. Zhang, F. Wang, J. Shi, P. Ci, L. Wang, L. Ge, S.Q. Wang, P.K. Chu, Three dimensional supercapacitors composed of Ba_{0.65}Sr_{0.35}TiO₃ (BST)/NiSi₂/silicon microchannel plates. *Mater. Sci. Eng. B.* **176**, 387–392 (2011)
15. C. Zhang, Y. Song, M. Wang, M. Yin, L. Tian, H. Wang, X. Chen, Z. Fan, L. Lu, D. Li, Efficient and Flexible thin film amorphous silicon solar cells on nanotextured polymer substrate using sol-gel based nanoimprinting method. *Adv. Funct. Mater.* **27**, 1604720 (2017)
16. K. Qiu, D. Qiu, L. Cai, S. Li, W. Wu, Z. Liang, H. Shen, Preparation of ZnS thin films and ZnS/p-Si heterojunction solar cells. *Mater. Lett.* **198**, 23–26 (2017)
17. S. Ferrari, M. Loveridge, S.D. Beattie, M. Jahn, R.J. Dashwood, R. Bhagat, Latest advances in the manufacturing of 3D rechargeable lithium Microbatteries. *J. Power Sources* **286**, 25–46 (2015)
18. S. Nohren, E. Quiroga-Gonzalez, J. Carstensen, Helmut Foll, electrochemical fabrication and characterization of silicon microwire anodes for Li ion batteries. *J. Electrochem. Soc.* **163**, A373–A379 (2016)
19. H. Porthault, F. Le Cras, J.M. Duffault, S. Franger, Fast deposition of conformal LiCoO₂ thin film electrodes for high capacity 3D batteries. *Mater. Sci. Eng. B* **213**, 163–168 (2016)
20. E. Eustache, C. Douard, A. Demortière, V. De Andrade, M. Brachet, J. Le Bideau, T. Brousse, C. Lethien, High areal energy 3D-interdigitated micro-supercapacitors in aqueous and ionic liquid electrolytes. *Adv. Mater. Technol.* **2**, 1700126 (2017)
21. M. Létiche, E. Eustache, J. Freixas, A. Demortière, V. De Andrade, L. Morgenroth, P. Tilmant, F. Vaurette, D. Troadec, P. Roussel, T. Brousse, C. Lethien, Atomic layer deposition of functional layers for on chip 3D Li-ion all solid state microbattery. *Adv. Energy Mater.* **7**, 1601402 (2017)
22. W.J. Lin, X. Qi, G. Chern, J.C.A. Huang, Epitaxial growth and exchange coupling of spinel ferrimagnet Ni_{0.3}Zn_{0.7}Fe₂O₄ on multiferroic BiFeO₃. *Thin Solid Films* **519**, 8326–8329 (2011)
23. Y.W. Li, Z.G. Hu, J.L. Sun, X.J. Meng, J.H. Chu, Effects of LaNiO₃ bottom electrode on structural and dielectric properties of CaCu₃Ti₄O₁₂ films fabricated by sol-gel method. *Appl. Phys. Lett.* **92**, 042901–042904 (2008)
24. G.P. Mambrini, E.R. Leite, M.T. Escote, A.J. Chiquito, E. Longo, J.A. Varela, R.F. Jardim, Structural, microstructural, and transport properties of highly oriented LaNiO₃ thin films deposited on SrTiO₃ (100) single crystal. *J. Appl. Phys.* **102**, 043708–043714 (2007)
25. R.W. Schwartz, Chemical solution deposition of perovskite thin films. *Am. Chem. Soc.* **9**, 2325–2340 (1997)
26. X. Meng, J. Cheng, J. Sun, H. Ye, S. Guo, J. Chu, Growth of (1 0 0)-oriented LaNiO₃ thin films directly on Si substrates by a simple metalorganic decomposition technique for the highly oriented PZT thin films. *J. Cryst. Growth* **220**, 100–104 (2000)
27. H. Miyazaki, T. Goto, Y. Miwa, T. Ohno, H. Suzuki, T. Ota, M. Takahashi, Preparation and evaluation of LaNiO₃ thin film electrode with chemical solution deposition. *J. Eur. Ceram. Soc.* **24**, 1005–1008 (2004)
28. A. Vincent, N. Poirot, Patent, Method depositing an inorganic material on a substrate, in particular a micron – or submicron – scale textured substrate WO/2015/044582 (2014)
29. Marie Gabard, Mustapha Zaghrioui, David Chouteau, Virginie Grimal, Thomas Tillocher, Fouad Ghamouss, Nathalie Poirot, Novel method based on spin-coating for the preparation of 2D and 3D Si-based anodes for lithium ion batteries. *Chem. Eng.* **1**, 5 (2017)
30. R. Dussart, T. Tillocher, P. Lefauchaux, M. Boufnichel, Plasma cryogenic etching of silicon: from the early days to today's advanced technologies. *Phys. D: Appl. Phys.* **47**, 123001–123028 (2014)
31. T. Tillocher, W. Kafrouni, J. Ladroue, P. Lefauchaux, M. Boufnichel, P. Ranson, R. Dussart, Optimization of submicron deep trench profiles with the STiGer cryo-etching process: reduction of defects. *J. Micromech. Microeng.* **21**, 085005–085014 (2011)
32. W. Kern, The evolution of silicon wafer cleaning technology. *J. Electrochem. Soc.* **137**, 1887–1892 (1990)
33. R. Seemann, M. Brinkmann, E.J. Kramer, F.F. Lange, R. Lipowsky, Wetting morphologies at microstructured surfaces. *PNAS* **102**, 1848–1852 (2005)
34. Y. Guo, D. Akai, K. Sawada, M. Ishida, Dielectric and ferroelectric properties of highly (100)-oriented (Na_{0.5}Bi_{0.5})_{0.94}Ba_{0.06}TiO₃ thin films grown on LaNiO₃/g-Al₂O₃/Si substrates by chemical solution deposition. *Solid State Sci.* **10**, 928–933 (2008)

Springer Nature or its licensor holds exclusive rights to this article under a publishing agreement with the author(s) or other rightsholder(s); author self-archiving of the accepted manuscript version of this article is solely governed by the terms of such publishing agreement and applicable law.